

Metallomacrocycles

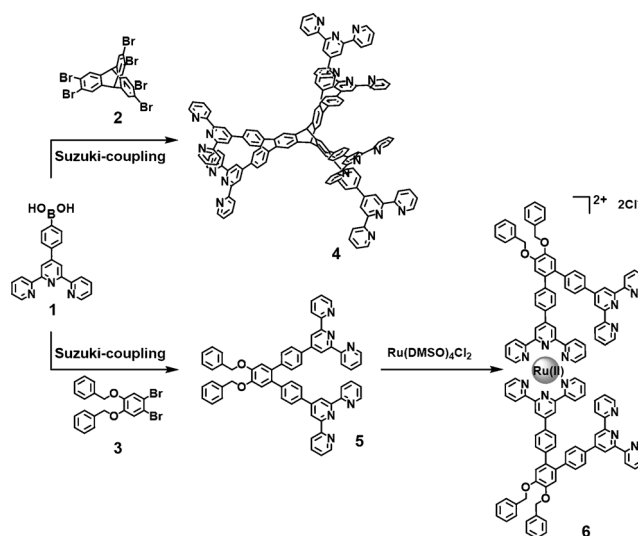
Towards Molecular Construction Platforms: Synthesis of a Metallotricyclic Spirane Based on Bis(2,2':6',2''-Terpyridine)Ru^{II} Connectivity

Ting-Zheng Xie,^[a] Kai Guo,^[a] Mingjun Huang,^[a] Xiaocun Lu,^[a] Sheng-Yun Liao,^[b] Rajarshi Sarkar,^[a] Charles N. Moorefield,^[a] Stephen Z. D. Cheng,^[a] Chrys Wesdemiotis,^{*[a]} and George R. Newkome^{*[a]}

Abstract: The design and construction of the first multi-component stepwise assembly of a < tpy-Ru^{II}-tpy >-based (tpy = terpyridine), three-dimensional, propeller-shaped trismacrocycle, **8**, are reported. Key steps in the synthesis involve the preparation of a hexaterpyridinyl triptycene and its reaction with dimeric, 60°-directional, bisterpyridine-Ru^{II} building blocks. Characterization includes ESI- and ESI-TWIM-MS and TEM, along with 1D and 2D ¹H NMR spectroscopy.

Inspiration arising from fascinating natural systems has long prodded synthetic chemists to mimic the shapes and properties of biomolecular scaffolds^[1] from which a wide variety of supramolecular structures has been investigated and developed.^[2] Many such constructs are predicated on molecular self-assembly, which is driven by precisely designed complementary components and, in many cases, employs noncovalent interactions.^[3] These protocols serve as the foundation for stepwise coordination-driven assembly, which can overcome entropic disadvantages and provide excellent avenues to nano- and macroscopic structures.^[4] In many cases, novel complex heteroleptic materials have been prepared.^[5,6]

Herein, we report the coordination-driven assembly of a nanoscopic, three-bladed, propeller-shaped spirane (**8**, Scheme 2) comprised of nine linear terpyridine-Ru^{II}-terpyridine (< tpy-Ru^{II}-tpy >) coordination linkages with architectures reminiscent of Meijere's^[7] and Kozhushkov's cyclopropane-based triangulanes. The metallotricycle **8** was obtained by the combination of two extended tpy ligands; a 60°-based < bisterpy-Ru^{II}-bisterpy > capping component and a triptycene-based hexakis-



Scheme 1. Syntheses of the hexakis(terpyridinyl) triptycene core **4** and the mono-Ru^{II} capping units **6**.

py core (**6** and **4**, respectively, Scheme 1). The critical hexakis(terpyridinyl) ligand employed for the core of the nanotricycle was constructed on a triptycene moiety that provided the requisite directionality exemplified in pseudorotaxanes.^[8] Previously reported < tpy-Ru^{II}-tpy >-constructed architectures possessing the triangular motif include triangle-based fibers,^[9] butterfly and bowtie spirane motifs,^[10] along with rhombic,^[11] and spoked-wheel metalocyclic structures.^[12] Construction of the metallospirane is thus predicated on this ubiquitous, stable, topological element.

Each dimeric capping unit possesses a central benzene ring connector that imposes a 60° angle between two attached terpyridines that is required for triangle formation.^[13] Preparation of the metallotricyclic spirane began with the synthesis of the triptycene-based core **4** (Scheme 1) that was accessed by a six-fold Suzuki-coupling reaction using the hexakisbromotriptycene **2** (prepared by a literature procedure^[14]) and 4-terpyridine-phenylboronic acid **1** (obtained from reaction of commercially available 4-formylphenylboronic acid with 2-acetyl pyridine and base, followed by NH₄OAc).^[12a] Isolation followed by column chromatography and recrystallization gave the desired hexadentate product **4** (60% yield). The ¹H NMR spectrum of **4** shows only one set of peaks for the tpy units, indicating

[a] Dr. T.-Z. Xie, K. Guo, M. Huang, Dr. X. Lu, R. Sarkar, Dr. C. N. Moorefield, Prof. S. Z. D. Cheng, Prof. C. Wesdemiotis, Prof. G. R. Newkome
Departments of Polymer Science and Chemistry and
The Maurice Morton Institute for Polymer Science
The University of Akron, Akron, OH 44325 (USA)
E-mail: wesdemiotis@uakron.edu
newkome@uakron.edu

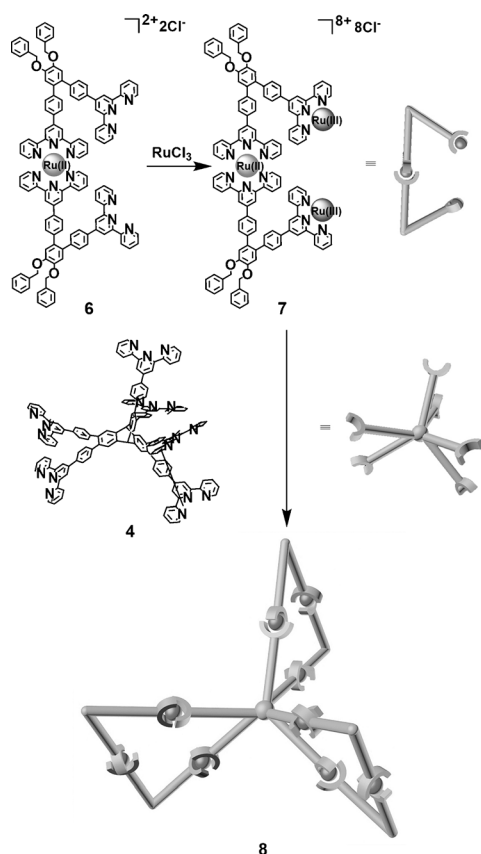
[b] S.-Y. Liao
Department of Chemistry, Nankai University, Tianjin, 300071 (P.R. China)

Supporting information for this article is available on the WWW under
<http://dx.doi.org/10.1002/chem.201403840>.

a single type of hexaterpyridinyl ligand as well as confirming its symmetric motif.

The monoRu^{II} terpyridinyl dimer **6** was synthesized from the dibenzyloxybisterpyridinylbenzene **5**, which was prepared by a two-fold Suzuki-coupling reaction utilizing dibromide **3** and 4-terpyridinylphenylboronic acid (**1**).^[10] Dimer **6** was isolated (65% yield) and used with chloride counterions to form the bisRu^{III} adduct **7**. Support for the formation of dimer **6** included the ¹H NMR spectrum, which revealed two singlets assigned to the protons of the benzyloxy methylene moieties at 5.30 and 5.29 ppm, indicating different diastereotopic environments after the formation of the Ru dimer. Two singlets observed at 9.37 and 8.73 ppm were assigned to the 3',5' protons from coordinated and non-coordinated terpyridine moieties, respectively. The peak at *m/z* 955.28 in the mass spectrum of **6** further supports its structure.

The paramagnetic bisRu^{III} adduct **7** of dimer **6** was synthesized (Scheme 2) by treatment with 3 equivalents of RuCl₃·*n*H₂O in EtOH heated at reflux, affording the capping



Scheme 2. Synthesis of the metallospirane nonacomplex **8**.

component for the polyspirane (98% yield). Subsequent treatment of the bisRu^{III} adduct **7** with the hexadentate triptycene **4** in a 3:1 ratio in the presence of *N*-ethylmorpholine in a mixture of MeOH and CHCl₃ (*v/v* 2:1) afforded a deep red solution upon heating at reflux for 24 h. Following column chromatography using silica, the pure product was isolated (30% yield) as the NO₃⁻ salt. The counterions were exchanged by employing

a saturated aqueous NH₄PF₆ solution to give the MeCN soluble complex [8(PF₆⁻)₁₈].

The ¹H NMR spectrum of this metallotricyclic spirocomplex **8** exhibited a set of peaks that were consistent with the formation of a discrete, symmetrical product. The *D*_{3h} symmetry of trispirane **8** arises from the arrangement of the three simple triangles that give rise to broadened absorptions owing to the three chemically non-equivalent terpyridinyl units exhibiting close chemical shifts. The ¹H NMR peaks assigned to the capping terpyridines nearly overlap and appear as a single broad peak (Figure 1). Where resolution permits, the terpyridinyl sig-

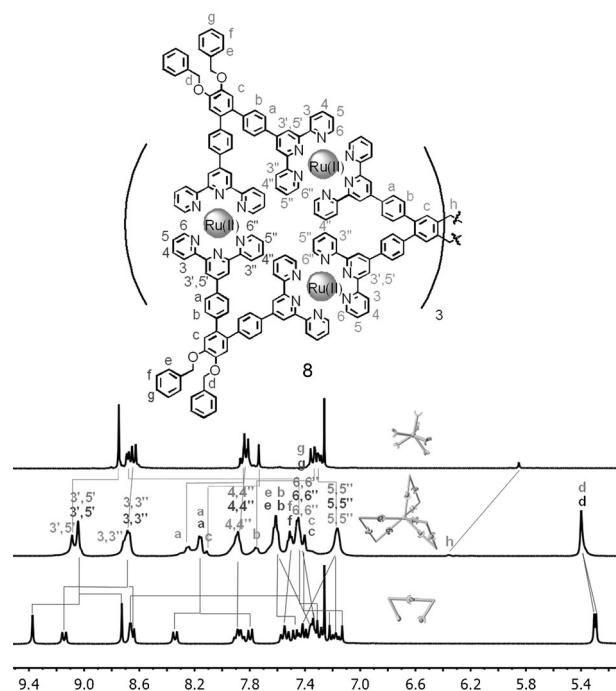


Figure 1. Stacked ¹H NMR spectra of the hexakisterpyridinyl core **4** (top), the metallospirane complex **8** (middle), and the bisRu^{III} bisterpyridine dimer **7** (bottom). Arrows depict assigned resonance shifts that occur upon complex formation.

nals appear as two sets of peaks in the ratio of 1:2, identifying the core and capping components, respectively. Thus, the 3',5' capping terpyridinyl protons appear together at 9.05 ppm and those attributed to the inner core terpyridines appear at 9.10 ppm. The protons attached to the tertiary carbon on the central triptycene unit are identified by a single peak at 6.36 ppm, further supporting the symmetry of this spirocomplex. A noticeable 0.51 ppm downfield shift of the triptycene moieties' tertiary C–H, compared with that of the metal-free core ligand **4**, was observed owing to a strong electropositive environment created by the proximity of nine Ru^{II} centers. Also notable, the benzyloxy methylene protons appear as a singlet and move slightly downfield to 5.39 ppm from approximately 5.30 ppm in the precursor. Assignment of all terpyridinyl and aromatic peaks was accomplished with NOESY and COSY experiments. For example, the 1D NMR broad signals arising from *H*^{tpy3,3'}, *H*^{tpy4,4'}, *H*^{tpy5,5'}, and *H*^{tpy6,6'} in **8** were assigned to

8.69, 7.89, 7.17, 7.45 ppm, respectively. The small singlet at 8.11 ppm was assigned to the $H_{C(\text{interior})}$ protons and the upfield shifted $H_{C(\text{outer})}$ protons assigned to 7.40 ppm.

The ESI-MS spectrum of the PF_6^- salt of the spirocomplex **8** with 18+ charges further confirms its structure (Figure 2a). A series of peaks ranging from m/z 591.59–1696.43 corresponds

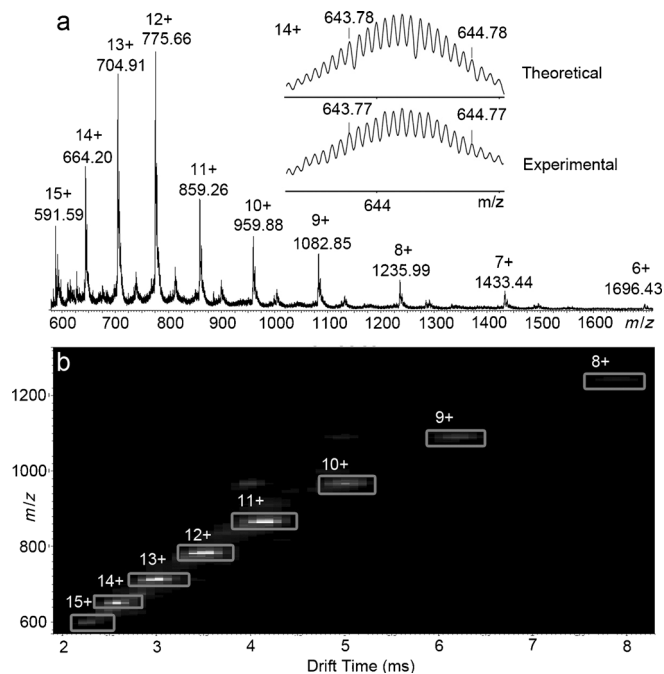


Figure 2. a) ESI-MS spectrum of complex **8**. Monoisotopic m/z values and charge states are marked on top of the corresponding peaks; the inset shows an expanded view of the measured and calculated isotope pattern for the 14+ ion. b) 2D ESI-TWIM-MS plot (m/z vs. drift time) of complex **8**. The charge states of intact assemblies are marked.

to the spirane cations possessing charge states from 15+ to 6+, respectively. In contrast to a related bowtie-shaped spirane,^[10] complex **8** exhibited fewer fragments in both the 1D and 2D ESI mass spectra, indicative of greater stability.

ESI-MS coupled with traveling-wave ion mobility (TWIM) spectrometry, a variant of ion mobility spectrometry,^[15] was applied to further validate the structure and to determine whether there are other conformers, based on differing drift times. The TWIM-MS spectrum of complex **8** (Figure 2b) reveals a set of narrow, symmetric peaks, confirming that there is only a single species existing in the solution under the conditions of ESI-MS. This is consistent with the NMR results. Compared with the multiple metal ion (≥ 6) macrocycles,^[16] this nanospirane exhibits the enhanced stability of the trigonal motif;^[9] gradient tandem MS (gMS^2)^[15a] was performed on the 12+ charge state (m/z 775.7) by subjecting it to collisionally activated dissociation prior to ion mobility separation at collision energies ranging from 10 to 40 eV. The 12+ complex ions dissociated completely when the trap voltage reached 35 V, which corresponds to a center-of-mass collision energy (E_{cm}) of 1.80 eV. This compares very well with the stability observed for other triangular constructs.^[9,11]

The computer-generated, energy-minimized structure of complex **8** also supports a rigid, shape-persistent, and highly symmetric spirane-shaped architecture with D_{3h} symmetry (Scheme 2). The distance between two Ru ions in an individual triangle is approximately 1.2 nm, whereas the distance between two Ru ions in adjacent triangles at the outer rim is approximately 4 nm. Same-side, corner-to-corner distances measure approximately 5.3 nm.

Further proof-of-structure was provided by determining the collision cross-section (CCS) of **8** from the drift times measured in the TWIM-MS experiments and comparing it with the theoretical CCS for 100 candidate structures obtained by molecular modeling. The CCSs measured for nanospirane ions in various charge states are listed in Table 1. Only slight fluctuations were

Table 1. Drift times and collision cross sections for the spirane.^[a]

Charge	Drift time [ms]	Collision cross section [\AA^2]
15+	2.71	1433
14+	2.44	1455
13+	2.89	1514
12+	3.34	1530
11+	3.97	1554
10+	4.87	1586
9+	6.05	1606

[a] All drift times were collected at a traveling-wave velocity of 350 m s^{-1} and a traveling-wave height of 7.5 V.

observed as the charge ranged from 15+ to 9+ ($1519 \pm 86 \text{ \AA}^2$), indicating rigidity and shape-persistence for the 3D-shaped architecture. Compared with the spoke-wheel metalloarchitecture,^[12] this 3D metalotricyclic spirane is only slightly smaller. The theoretical CCS calculated by the trajectory (TJ) method^[17] for the energy-minimized structure of **8** (no counterions) is 1580 \AA^2 ; this value agrees well with the average experimental CCS for charge states 9+ to 15+ (1519 \AA^2).

Notably, the use of Zn^{II} or Cd^{II} ions, as in the synthesis of our isomeric supramolecular bowtie and butterfly structures^[10] with ester substituted Ru^{II} -based capping dimers and tetraterpyridinyl cores, afforded a substantial amount the corresponding cyclic tetramer^[13] as a byproduct (as determined by $^1\text{H NMR}$).

Transmission electron microscopy (TEM) experiments have facilitated visualization of spirane **8** (Figure 3). The TEM images revealed direct correlation of both size and shape of individual molecules upon deposition of a dilute ($\sim 10^{-7} \text{ M}$) MeCN solution of complex **8** with PF_6^- counterions on carbon-coated grids (Cu, 400 mesh). The outline of single molecules located on the film with three triangles vertically erected can be observed; a slight tilt of the molecule also shows the structure's concave side. The average distance (5.3 nm) between the two edges perfectly fits the size obtained from the optimized molecular model.

In conclusion, we have developed a novel all- Ru^{II} polyspirane-shaped metallomacrocyclic through programmed coordination-driven assembly based on the logical combination of

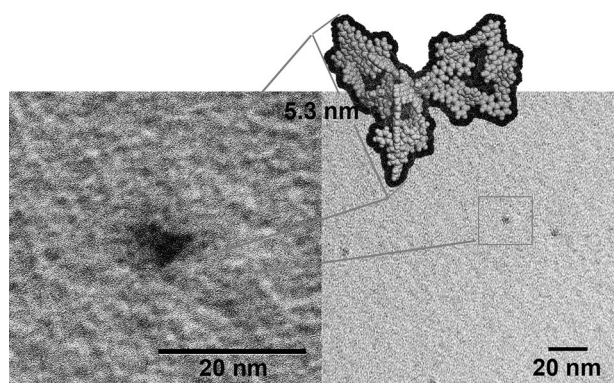


Figure 3. TEM images of complex **8** obtained on a carbon-coated Cu grid and a representative, computer-generated, energy-minimized structure of spirane **8**.

nine Ru^{II} metal ions, six bidentate- and one hexadentate terpyridinyl ligands. The pedestal-like complex has been characterized by ESI-MS, TWIM-MS, ¹H NMR, 2D COSY, and NOESY NMR, as well as computer-generated modeling. Incorporation of an extended dimeric monoRu^{II} building block facilitates metallocyclic construction by reducing the degrees-of-freedom in the product outcome. Application of similar synthetic protocols with predesigned elements is envisioned to permit the construction of other novel 3D materials. Investigations with these and similar platforms are ongoing.

Acknowledgements

The authors gratefully acknowledge funding from the National Science Foundation [CHE-1151991 (GRN) and CHE-1012636 and CHE-1308307 (CW)].

Keywords: metallomacrocycles · ruthenium · self-assembly · spiranes · terpyridine

- [1] a) J.-M. Lehn, *Supramolecular Chemistry: Concepts and Perspectives*, Wiley-VCH, Weinheim, **1995**; b) W. R. Wikoff, L. Liljas, R. L. Duda, H. Tsuruta, R. W. Hendrix, J. E. Johnson, *Science* **2000**, *289*, 2129–2133; c) J.-M. Lehn, *Science* **2002**, *295*, 2400–2403; d) G. M. Whitesides, B. Grzybowski, *Science* **2002**, *295*, 2418–2421.
- [2] a) J. P. Sauvage, P. Gaspard, *Non-Covalent Assemblies to Molecular Machines*, Wiley-VCH, Weinheim, **2010**; b) R. S. Forgan, J.-P. Sauvage, J. F. Stoddart, *Chem. Rev.* **2011**, *111*, 5434–5464; c) E. C. Constable, *Coord. Chem. Rev.* **2008**, *252*, 842–855.

- [3] a) M. Fujita, M. Tominaga, A. Hori, B. Therrien, *Acc. Chem. Res.* **2005**, *38*, 369–378; b) T. R. Cook, Y.-R. Zheng, P. J. Stang, *Chem. Rev.* **2013**, *113*, 734–777; c) R. Bhola, P. Payamyar, D. J. Murray, B. Kumar, A. J. Teator, M. U. Schmidt, S. M. Hammer, A. Saha, J. Sakamoto, A. D. Schlüter, B. T. King, *J. Am. Chem. Soc.* **2013**, *135*, 14134–14141; d) C. Grave, D. Lentz, A. Schäfer, P. Samori, J. P. Rabe, P. Franke, A. D. Schlüter, *J. Am. Chem. Soc.* **2003**, *125*, 6907–6918; e) T. Bauer, Z. Zheng, A. Renn, R. Enning, A. Stemmer, J. Sakamoto, A. D. Schlüter, *Angew. Chem.* **2011**, *123*, 8025–8030; *Angew. Chem. Int. Ed.* **2011**, *50*, 7879–7884.
- [4] a) M. M. Ali, F. M. MacDonnell, *J. Am. Chem. Soc.* **2000**, *122*, 11527–11528; b) E. Iengo, E. Zangrando, R. Minatel, E. Alessio, *J. Am. Chem. Soc.* **2002**, *124*, 1003–1013; c) H. Jiang, W. Lin, *J. Am. Chem. Soc.* **2006**, *128*, 11286–11297; d) A. Barbieria, B. Ventura, R. Ziessel, *Coord. Chem. Rev.* **2012**, *256*, 1732–1741.
- [5] G. R. Newkome, P. Wang, C. N. Moorefield, T. J. Cho, P. P. Mohapatra, S. Li, S.-H. Hwang, O. Lukoyanova, L. Echevoyen, J. A. Palagallo, V. Iancu, S.-W. Hla, *Science* **2006**, *312*, 1782–1785.
- [6] a) S. De, K. Mahata, M. Schmittel, *Chem. Soc. Rev.* **2010**, *39*, 1555–1575; b) M. Schmittel, K. Mahata, *Chem. Commun.* **2010**, *46*, 4163–4165; c) K. Mahata, M. Schmittel, *J. Am. Chem. Soc.* **2009**, *131*, 16544–16554; d) M. Schmittel, B. He, P. Mal, *Org. Lett.* **2008**, *10*, 2513–2516.
- [7] A. de Meijere, S. I. Kozhushkov, *Chem. Rev.* **2000**, *100*, 93–142.
- [8] X.-Z. Zhu, C.-F. Chen, *J. Am. Chem. Soc.* **2005**, *127*, 13158–13159.
- [9] A. Schultz, Y. Cao, M. Huang, S. Z. D. Cheng, X. Li, C. N. Moorefield, C. Wesdemiotis, G. R. Newkome, *Dalton Trans.* **2012**, *41*, 11573–11575.
- [10] A. Schultz, X. Li, B. Barkakaty, C. N. Moorefield, C. Wesdemiotis, G. R. Newkome, *J. Am. Chem. Soc.* **2012**, *134*, 7672–7675.
- [11] X. Lu, X. Li, J.-L.; Wang, X. Li, X. Lu, I.-F. Hsieh, Y. Cao, C. N. Moorefield, C. Wesdemiotis, S. Z. D. Cheng, G. R. Newkome, *J. Am. Chem. Soc.* **2011**, *133*, 11450–11453; Wang, C. N. Moorefield, C. Wesdemiotis, G. R. Newkome, *Chem. Commun.* **2012**, *48*, 9873–9875.
- [12] a) J.-L.; Wang, X. Li, X. Lu, I.-F. Hsieh, Y. Cao, C. N. Moorefield, C. Wesdemiotis, S. Z. D. Cheng, G. R. Newkome, *J. Am. Chem. Soc.* **2011**, *133*, 11450–11453; b) X. Lu, X. Li, Y. Cao, A. Schultz, J.-L. Wang, C. N. Moorefield, C. Wesdemiotis, S. Z. D. Cheng, G. R. Newkome, *Angew. Chem.* **2013**, *125*, 7882–7885; *Angew. Chem. Int. Ed.* **2013**, *52*, 7728–7731.
- [13] A. Schultz, X. Li, C. N. Moorefield, C. Wesdemiotis, G. R. Newkome, *Eur. J. Inorg. Chem.* **2013**, *14*, 2492–2497.
- [14] K. A. Williams, C. W. Bielawski, *Chem. Commun.* **2010**, *46*, 5166–5168.
- [15] a) X. Li, Y.-T. Chan, G. R. Newkome, C. Wesdemiotis, *Anal. Chem.* **2011**, *83*, 1284–1290; b) S. Perera, X. Li, M. Soler, A. Schultz, C. Wesdemiotis, C. N. Moorefield, G. R. Newkome, *Angew. Chem.* **2010**, *122*, 6689–6694; *Angew. Chem. Int. Ed.* **2010**, *49*, 6539–6544; c) C. S. Hoaglund-Hyzer, A. E. Counterman, D. E. Clemmer, *Chem. Rev.* **1999**, *99*, 3037–3079; d) E. R. Brocker, S. E. Anderson, B. H. Northrop, P. J. Stang, M. T. Bowers, *J. Am. Chem. Soc.* **2010**, *132*, 13486–13494.
- [16] Y.-T. Chan, X. Li, C. N. Moorefield, C. Wesdemiotis, G. R. Newkome, *Chem. Eur. J.* **2011**, *17*, 7750–7754.
- [17] a) A. A. Shvartsburg, M. F. Jarrold, *Chem. Phys. Lett.* **1996**, *261*, 86–91; b) M. F. Jarrold, *Annu. Rev. Phys. Chem.* **2000**, *51*, 179–207; c) A. A. Shvartsburg, B. Liu, K. W. M. Siu, K.-M. Ho, *J. Phys. Chem. A* **2000**, *104*, 6152–6157.

Received: June 6, 2014

Published online on July 23, 2014